

Large-Scale Computational Modeling of H5 Influenza Variants Against HA1-Neutralizing Antibodies

Colby T. Ford^{1,2,3,4}, Shirish Yasa^{1,2}, Khaled Obeid^{1,2}, Rafael Jaimes III⁵, Phillip J. Tomezsko⁵, Sayal Guirales-Medrano^{1,2}, Richard Allen White III^{1,2,6}, and Daniel Janies^{1,2,6}✉

¹University of North Carolina at Charlotte, Center for Computational Intelligence to Predict Health and Environmental Risks (CIPHER), Charlotte, NC, USA

²University of North Carolina at Charlotte, Department of Bioinformatics and Genomics, Charlotte, NC, USA

³University of North Carolina at Charlotte, School of Data Science, Charlotte, NC, USA

⁴Tuple LLC, Charlotte, NC, USA

⁵Massachusetts Institute of Technology, Cambridge, MA, USA

⁶North Carolina Research Campus (NCRC), Kannapolis, NC, USA

Abstract

The United States Department of Agriculture has recently released reports that show samples from 2022-2024 of highly pathogenic avian influenza (H5N1) have been detected in mammals and birds (1). To date, the United States Centers for Disease Control reports that there have been 27 humans infected with H5N1 in 2024 (2). The broader potential impact on human health remains unclear. In this study, we computationally model 1,804 protein complexes consisting of various H5 isolates from 1959 to 2024 against 11 hemagglutinin domain 1 (HA1)-neutralizing antibodies. This study shows a trend of weakening binding affinity of existing antibodies against H5 isolates over time, indicating that the H5N1 virus is evolving immune escape of our medical defenses. We also found that based on the wide variety of host species and geographic locations in which H5N1 was observed to have been transmitted from birds to mammals, there is not a single central reservoir host species or location associated with H5N1's spread. These results indicate that the virus has potential to move from epidemic to pandemic status in the near future. This study illustrates the value of high-performance computing to rapidly model protein-protein interactions and viral genomic sequence data at-scale for functional insights into medical preparedness.

influenza | H5 | antibodies | protein modeling | docking | zoonosis

Correspondence: djanies@charlotte.edu

Research in Context

Evidence before this study. Previous studies have shown cases of avian influenza transmissions to mammals that are increasing in frequency, which is of concern to human health. Since 1997, nearly a thousand H5N1 cases have been reported in humans with a 52% fatality rate. Previous analyses have indicated specific mutations on the hemagglutinin protein that allow for this "host jumping" between birds and mammals (3). There are also existing evidence of recent viral strains with reduced neutralization to sera (4).

Added value of this study. This study provides a comprehensive look at the mutational space of hemagglutinin of H5N1 influenza and presents computational predictions of the binding between various HA1-neutralizing antibodies derived from infected vaccinated patients and humanized mice and 1,804 representative H5 HA1 proteins. These analyses show a weakening trend of existing antibodies. We also confirm that the mutations found in other studies that enable zoonosis also affect binding affinities of the antibodies tested.

Furthermore, through phylogenetic analyses, we quantify the avian-to-mammalian transmissions from 1959 to 2024 and show a persistent circulation of isolates between North America and Europe.

Taken together, the continuous transmission of H5N1 from birds to mammals and the increase in immuno-evasive HA strains in mammals sampled over time suggest that antigenic drift is a source of spillover risk.

Implications of all the available evidence. Our findings indicate that the worsening in antibody binding, along with the increase in of avian-to-mammalian H5N1 influenza transmissions are risks to public health.

Through the findings of previous studies along with the predictions reported in this study, we can now monitor specific mutations of interest, quantified by their potential impact on antibody evasion, and inform public health monitoring of circulating isolates in 2024 and beyond.

In addition, these findings may help to guide future vaccine and therapeutic development in the fight against H5N1 influenza infections in humans.

Introduction

Wild aquatic birds (e.g., order Anseriformes) are fundamental hosts of influenza viruses, which are transmitted from domestic birds (e.g., Galliformes) and mammals (orders Artiodactyla, Carnivora, and Primates) (5, 6). H5N1 has circulated in nature since 1959, following an outbreak in Scotland in chickens (7). In 1996, H5N1 influenza largely occurred in Anseriformes and spread to humans and chickens in Hong Kong in 1997 (6, 8). As a response to H5N1 in chickens and occasional human infection, chickens were culled in Hong Kong in the period 1997 to 2011 (9). In 2002, the most common hosts of H5N1 were Anseriformes with occasional transmission to Galliformes and humans throughout China and South East Asia (6, 10). Since 2003, various lineages of H5N1 have spread throughout China and Hong Kong, South East Asia, Russia, North Africa, the West Bank, Gaza Strip and Israel, Pakistan, Bangladesh, India, Bhutan, Nepal, Europe, Japan and South Korea, using a wide variety of hosts (11, 12). Many avian taxa (Charadriiformes, Accipitriformes, Corvidae, Ardeidae, Columbidae, and Passeriformes) as well as primate, carnivore, artiodactyl, and arthropod hosts have been infected with H5N1 (6). H5N1 infections in humans have been reported by the World Health Organization (WHO) in: Hong Kong 1997–2003, in China and Hong Kong 2003–2014; in Thailand 2003–2007; in Indonesia 2005–2012; in Nigeria in 2007; in Bangladesh 2011–2013; in Azerbaijan, Turkey, Iraq, Myanmar, Pakistan, and Djibouti in 2006–2007; in Egypt 2003–2014; in Lao PDR 2007; in Vietnam 2003–2014; in Cambodia 2003–2014, and in Canada in 2014. The document produced by the WHO has not been updated since (13).

However, a comprehensive review from 2023 (14) illustrates the recent (2022–23) spread (on top of the previous spread) of H5N1 in animals as follows:

- **Asia:** Bhutan, Hong Kong, India, Japan, Korea, Nepal, Philippines, Taiwan, and Vietnam.
- **Europe:** Albania, Austria, Belgium, Bosnia and Herzegovina, Bulgaria, Croatia, Czechia, Denmark, Estonia, Finland, France, Germany, Greece, Hungary, Iceland, Ireland, Italy, Latvia, Lithuania, Luxembourg, Moldova, Montenegro, Netherlands, North Macedonia, Norway, Poland, Portugal, Romania, Russia, Serbia, Slovakia, Slovenia, Spain, Sweden, Switzerland, and the United Kingdom.
- **The Middle East:** Israel and Turkey.
- **Africa:** Algeria, Gambia, Nigeria, Reunion, Senegal, and South Africa.
- **North and South America:** Bolivia, Brazil, Canada, Bolivia, Chile, Colombia, Ecuador, Guatemala, Honduras, Mexico, Panama, Peru, Venezuela, and the United States.

In 2024, H5N1 has been found in animals in Antarctica (15). Also, in March 2024, an outbreak of H5N1 was reported among several herds of U.S. dairy cattle. H5N1 also caused fatal infections among cats, infection in poultry, and four reported infections in dairy workers (16–18). From 1997 to late April 2024, 909 human H5N1 cases were reported, with 52% of cases being fatal (19).

Continued transmission of avian strains of H5N1 to livestock and humans may lead to subsequent human-to-human transmission which can devastate public health world-

wide. As the human-animal interface increases due to shrinking natural habitats, deforestation, and increased demand for animal products; animal-human disease transmission is becoming more common (20).

Current human seasonal influenza vaccines do not confer immunity against H5N1 influenza or other animal influenza A viruses (21). Moreover, recent studies have shown there is little existing immunity to H5N1 in the USA (22). Such immunity may exist elsewhere in the world and in populations in due to previous infection or immunization.

Thus, it is of great public health interest to discover rapidly develop molecular insight into the effects of mutations of H5N1 on existing human immunity (23). In this study, we present the results of a large computational corpus of molecular docking experiments between various H5 isolates against existing HA1-neutralizing antibodies and show changes over time.

Methods

This study closely follows the published methods in Tomezsko and Ford et al. (2024) and other protein modeling studies by this team (25–29). The specific workflow for this study is depicted in Figure 1.

HA1 Sequence Collection. 18,693 influenza A H5 sequences were downloaded from the GISAID EpiFlu database (30, 31) on June 17, 2024. Isolate metadata, including: date of viral isolation, country of origin, and host information, were also collected. We then derived taxonomic classifications from the provided host metadata along with continent of origin from the country information.

These amino acid sequences were clustered using CD-HIT v4.8.1 (32, 33). Ranging in size from 11 to 576 amino acids, the process resulted in 250 clusters, based on 97% identity. A representative sequence from each of these clusters was selected, which was then output in a FASTA file.

These representative sequences were then aligned to each other with MUSCLE v3.8.425 (34) using default settings. Then, sequences that were of low quality, incomplete, or did not contain the desired hemagglutinin domain 1 (HA1) region were removed. This resulted in 164 amino acid sequences that were used in the subsequent steps. These sequences were trimmed to the HA1 receptor binding domain (approximately residues 111–269, depending on the presence of indels) (35).

Also, clusters consisting of only lab derived isolates ($n = 3$) were analyzed, but have been left out of the reported statistics and visualizations.

Structure Prediction. Structures for each of the 164 HA1 sequences were predicted using ColabFold v1.5.5 (36), a protein folding framework that uses AlphaFold2 (37) accelerated with MMseqs2 (38), with default settings. The side chains of these predicted structures were relaxed using the OpenMM/Amber method (39). The .PDB file output of the

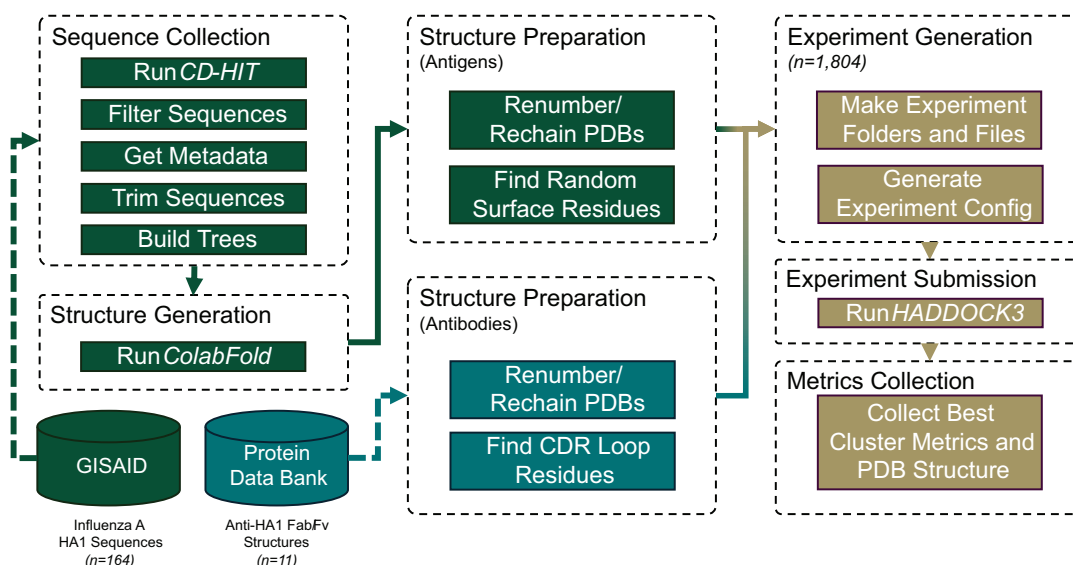


Fig. 1. Workflow diagram of the data procurement, data preparation, and analysis steps.

top structure (i.e., the one with the highest pLDDT¹ confidence) was selected and used for subsequent analyses.

Neutralizing Antibody Collection. Existing structures for 11 HA1-neutralizing antibodies were collected by a database search through Thera-SABdab (40) and the Protein Data Bank (41). Each of these 11 antibody structures have an epitope on the target HA1 domain of the hemagglutinin protein, though not all share the same epitope. These antibodies and their respective PDB IDs are listed in Table 1.

| Antibody ID | PDB ID | Year (Reference) | Clade | H/L Chain Subgroups | Source Information |
|-------------|--------|------------------|----------|---------------------|---|
| 100F4 | 5dur | 2015 (42) | 2.3.4.4 | II/I | Human Memory B-Cell, Recovered from H5N1 Infection |
| 12H5 | 7fah | 2022 (43) | 2.3.4.4 | I/IV | Mouse, Immunized with three H1N1 strains, Humanized |
| 13D4 | 6a0z | 2018 (44) | 2.3.2.1c | II/I | Mouse, Immunized with five H5N1 strains, Humanized |
| 3C11 | 6iuv | 2019 (45) | 2.3.4.4 | I/II | Human Memory B-cell, Infected by H5N1 viruses |
| 65C6 | 5dum | 2015 (42) | 2.3.4.4 | I/III | Human, Infected by H5N1 viruses |
| AVFlulg01 | 6iut | 2019 (45) | 2.3.4.4 | II/I | Human, Infected by H5N1 viruses |
| AVFlulg03 | 5dup | 2015 (42) | 2.3.4.4 | III/I | Human, Infected by H5N1 viruses |
| FLD194 | 5a3i | 2015 (46) | 2.3.4.4 | II/I | Human Memory B-cell, Recovered from H5N1 infection |
| FLD21.140 | 6a67 | 2018 (47) | 2.3.4.4 | ?/I | Human, Recovered from H5N1 Infection |
| H5M9 | 4mhh | 2013 (48) | 2.3.2.1 | I/IV | Mouse, Immunized with H5N1, Humanized |
| H5.3 | 4xrc | 2015 (49) | 2.3.4.4 | II/? | Human, Immunized with one H5N1 strain |

Table 1. HA1-neutralizing antibodies.

Docking Analyses. Using HADDOCK3, a computational framework for the integrative modeling of biomolecular complexes (50), each antibody was docked to each antigen across the dataset. Given the 11 antibody structures and 164 HA1

structures, this resulted in 1,804 docking experiments to be performed.

Experiment Generation. HADDOCK3 inputs for each experiment were generated programmatically, defining the antibody and antigen .PDB file inputs on which to dock. Other experiment files were also copied or created programmatically including the scripts to run the docking process and to generate other configuration files.

HADDOCK3 requires the definition of active and inactive residue restraints (AIRs) to help guide the protein docking process. To avoid biasing the docking placement of the antibody on the HA1 antigens, a random subset of surface residues were selected as “active” and were then included in the AIR file on which to dock. For the antibody structures, residues in the CDR loops were detected using ANARCI (51), a Python package for numbering antibody sequences.

Lastly, HADDOCK3 configuration files were generated programmatically, which define the input .PDB files, the output directory, and the steps of the docking process. The logic for this programmatic generation of HADDOCK3 configuration files is available in the supplementary GitHub repository.

Docking Process. HADDOCK3 provides a configurable interface for defining the individual steps of the docking process, including the rigid-body docking, flexible refinement, and solvent-based refinement, along with any desired clustering and filtering steps.

For this study, we customized the published HADDOCK3 protocol for antibody-antigen modeling (52) to focus on generating the singular best cluster of docking results for each experiment and reducing excess work by the docking process. The specific steps of our HADDOCK3 configuration that was used for the experiments are shown in Table 2.

¹Predicted local distance difference test (pLDDT): An estimate of local confidence, scaled from [0, 100], where higher scores indicate higher confidence in the protein conformation.

| Step | Description | # Models |
|------|--|----------|
| 1 | Topology Modeling | - |
| 2 | Rigid Body Modeling $n = 200$ | 200 |
| 3 | Cluster with FCC | 200 |
| 4 | Select Top Clusters $n = 5, m = 10$ | 50 |
| 5 | Flexible Refinement | 50 |
| 6 | Cluster with FCC | 50 |
| 7 | Select Top Cluster $n = 1, m = 10$ | 10 |
| 8 | Solvent Refinement | 10 |
| 9 | Molecular Dynamics Scoring | 10 |
| 10 | Cluster with FCC | ~10 |
| 11 | Calculate CAPRI Metrics | ~10 |

Table 2. Descriptions of the steps of the HADDOCK3 docking configuration.

The HADDOCK3 system outputs multiple metrics for the predicted binding affinities and an output set of PDB files containing the antibody docked against the HA1 antigen. Some main metrics include:

- Van der Waals intermolecular energy (*vdw*)
- Electrostatic intermolecular energy (*elec*)
- Desolvation energy (*desolv*)
- Restraints violation energy (*air*)
- Buried surface area (*bsa*)
- Total energy (*total*): $1.0vdw + 1.0elec$
- HADDOCK score: $1.0vdw + 0.2elec + 1.0desolv + 0.1air$

Note that the HADDOCK Score is a conglomerate metric used to assess the best complexes (or best cluster of complexes) that get promoted through the various refinement iterations in the pipeline.

Computational Scalability. For this study, we used a Docker containerized version of HADDOCK3^{2,3}, which contains all of the software dependencies to allow HADDOCK3 to run more readily in a high-performance computing (HPC) environment.

HADDOCK3 was run in a Singularity container on the UNC Charlotte Orion HPC cluster on 14 nodes, each with dual 18-core Intel Xeon Gold 6154 3.00GHz CPUs (36 cores per node). The average walltime of the experiments was 14.6 $\bar{3}$ minutes. The entire set of 1,804 experiments was completed in under 2 days.

Post Processing. Once all experiments were completed, the metrics for each experiment were either retrieved from the CAPRI evaluation outputs (if the FCC clustering algorithm (53) reached convergence) or from the REMARK entries of the best cluster's .PDB files. These metrics were organized in a single aggregate table, representing each experiment's best cluster metrics, for subsequent visualization and statistical analyses. The full table of experiment results is available in the Supplementary Data.

Phylogenetic, Statistical, and Protein Structure Analyses.

For phylogenetic analyses, laboratory derived isolates were filtered out ($n = 178$, shown in Table 3), resulting in a set of 18,515 isolates. An alignment 18,515 HA sequences was generated using MAFFT

²Container GitHub Repository: <https://github.com/colbyford/HADDOCKer>

³Docker Hub Images: <https://hub.docker.com/r/cford38/haddock>

v7.471 (54) under default settings. Next, a phylogenetic tree search was performed using this alignment with TNT v1.6 (55) using the commands: `xmult= level 1 rep 1000`. One of the best scoring trees was used for downstream analyses. StrainHub v2.0.0 (56) was used to generate transmission networks of the phylogenetic tree by host class and continent in Figure 2.

Statistical analyses were performed using R v4.3.4 (57) and plots were generated using ggplot2 (58) and ggpubr (59). Any statistical significance reported in this study is based on a p-value threshold of $\alpha < 0.05$.

Visualizations and analyses of the protein complexes were generated using PyMOL v2.4.1 (60) and BioPandas v0.4.1 (61).

Graph-based Interface Residue Assessment. Graph-based interface residue assessment function (GIRAF) was employed to evaluate the evolution of the binding pocket with each antibody as previously described (24). The outgroup was first selected as sequence EPI242227, and a graph was computed based on the interface residues with each antibody to generate reference complexes. Subsequent graphs were then computed for each strain sequence and antibody pair. The graph edit distance (GED) was computed as the number of edits to the strain:antibody complex from the reference outgroup:antibody complex. Substitutions, deletions, and additions, were all equally weighted as a value of "1".

Ethics Statement. No human or animal samples were used in this study. This study was conducted in accordance with the data usage guidelines of GISAID and the research ethics policies of the University of North Carolina at Charlotte.

Role of Funders. No external funders were used in this study and thus played no role in the study design, data collection, data analyses, interpretation, or writing of the manuscript.

Results

From the study set of 18,693 H5 isolates, we show a breakdown of hosts similar to what has been reported in previous studies, indicating the representative nature of our curated dataset (5, 6). As shown in Table 3, approximately 88% of the isolates are from birds (class Aves). Also, note that all 666 isolates from Primates were collected from humans.

| Class | Order | Isolates | % of Total |
|--------------------|-----------------------|---------------|---------------|
| Aves | Galliformes | 5,844 | 31.26% |
| | Anseriformes | 4,469 | 23.91% |
| | Other Orders | 934 | 5.00% |
| | Not Specified | 5,287 | 28.28% |
| | <i>Aves Total</i> | <i>16,534</i> | <i>88.45%</i> |
| Mammalia | Primates (Humans) | 666 | 3.56% |
| | Carnivora | 191 | 1.02% |
| | Artiodactyla | 57 | 0.30% |
| | Other Orders | 6 | 0.03% |
| | Not Specified | 360 | 1.93% |
| | <i>Mammalia Total</i> | <i>1,280</i> | <i>6.85%</i> |
| Insecta | <i>Insecta Total</i> | <i>3</i> | <i>0.02%</i> |
| Other | Laboratory Derived | 178 | 0.95% |
| | Other / Environmental | 698 | 3.73% |
| | <i>Other Total</i> | <i>876</i> | <i>4.69%</i> |
| Grand Total | | 18,693 | 100% |

Table 3. Taxonomic breakdown of the isolates used in this study.

As shown in Supplementary Figure 2, the proportion of H5 isolates collected from various continents has changed over time. To date, isolates collected in 2024 are predominately from Europe.

Sequence Analyses. The clustering of the 18,693 HA1 sequences resulted in 250 distinct clusters at $\geq 97\%$ identity. Further organization of the representative sequences of each cluster, shown in Supplementary Figure 3, indicates a continuous distribution of antibody binding performance.

Of note, antibodies 12H5, 3C11, 65C6, AVFluIgG01, and H5M9 show the best performance overall, though there are exceptions of poor performance (e.g., 12H5's interaction with EPI893474 has a poor Van der Waals energy of -39.93).

Phylogenetic and Transmission Network Analyses. Specifically, the most common pattern is avian-to-mammalian transmission, of which there are over 600 events across the tree (see Figure 2a). There are also frequent transmission events between many continents. Bidirectional transmissions between Europe and North America are very frequent as shown by the thick orange and yellow lines in Figure 2b.

Worsening Binding Affinity. When considering a past-to-present trend in viral collection date, there are significant correlations that show a worsening in antibody binding affinity in isolates collected from humans. See Figure 3. This worsening in binding affinity is not specific to particular antibodies. Though the antibodies' performances are from independent distributions, as shown by the Kruskal-Wallis test in Supplementary Figure 4, the overall trend indicates that more recent isolates have mutated to better evade existing antibodies (antibodies that were previously elicited by vaccination or infection or developed for therapeutic usage).

As shown in Figure 4A, there is no overall trend in the graph edit distance of the isolates over time. In other words, when comparing to the 1959 isolate, EPI242227, interactions are not necessarily more or less abundant in more recent isolates than older ones overall.

As shown in Figure 4C, we see a statistically significant decreases of interfacing residues over time in antibodies AVFluIgF01 against human isolates. Conversely, we see a statistically significant increase in interfacing residues in FLD194 against human residues.

These results indicate an overall worsening in antibody affinity to more recent H5N1 isolates, which poses a risk to public health

in that the virus may evade existing antibodies and risk the development of severe sickness in humans.

Mutational Effects. As indicated in Shi et al. (2014), there are various sites in the HA1 receptor binding domain that enable infection of mammals when mutated. Our results show several statistically significant differences in the binding affinity of antibodies given polymorphism at sites that allow mammalian infection.

Of note, N158S, T160A/S/V, E190N, and G225R all result in weakened antibody binding affinity across multiple metrics. Conversely, T160K and G228S increase binding affinity in some metrics. Significant changes based in Van der Waals energies and HADDOCK Scores are shown in Figure 6 and all other metrics are shown in Supplementary Figure 5.

In Figure 5, subfigures A and B represent the worst and best binding structures across the experimental results, isolates EPI168674 and EPI2429052, respectively. Though the epitope is different between isolates, note the variation in quantity of polar contacts within the respective complexes. Figure 5D is an example of modest binding affinity between an isolate EPI658567 and antibody 12H5. However, this improved binding affinity compared to other isolates is not due to the G225R mutation as this residue is not in the epitope of the antigen.

Figure 5E shows the poor binding affinity of isolate EPI3178330 with antibody FLD194 due to the E190N mutation. However, this residue forms a polar contact with the antibody CDR loop. The mutation from glutamic acid (E), a negatively charged side chain, to asparagine (N), a polar uncharged side chain.

Isolate EPI242227 is the oldest isolate in the dataset, collected in 1959. Note that this isolate contains the N158D mutation and its interaction with various antibodies results in a wide range of Van der Waals energies from -52.81 (worst) to -92.84 (best, with antibody 65C3 as shown in Figure 5F).

Interfacing Residue Prevalence. An analysis of the interfacing residues in the best complexes from all 1,804 experiments shows patterns in particular residues forming polar contacts with the antibodies tested. Residues 156, 193, 222 are often interfaced ($\geq 25\%$ prevalence) in the antigen epitope. These are shown in red in Figure 7.

Many of the frequently interfaced residues shown in this study closely neighbor antigenic and receptor binding sites reported in Sriwilajaroen and Suzuki (2012) Figure 2. Residues 130, 132, 158, and 159 are part of two glycosylation sites that, in 2012, were only found in seasonal H1 viruses (35).

Discussion

Relation to Prior Studies. This *in silico* analysis yields the trend of a reduction in binding affinity for neutralizing antibodies against H5N1-designated influenza isolates. This reduction in binding affinity reinforces previous studies that evolution has occurred to yield HA proteins that are elusive of antibody neutralization (62, 63). The trend observed is consistent with empirical studies and strengthens the novel *in silico* approach taken within this study. Current bio-surveillance efforts focus on critical mutations that have been shown to increase virulence or transmission risk, such as those included in the influenza risk assessment framework (IRAF) (64). This work suggests that the current arsenal of broadly neutralizing antibodies against H5N1 is becoming increasingly insufficient as H5N1 evolves, indicating a need for more studies to identify effective antibodies.

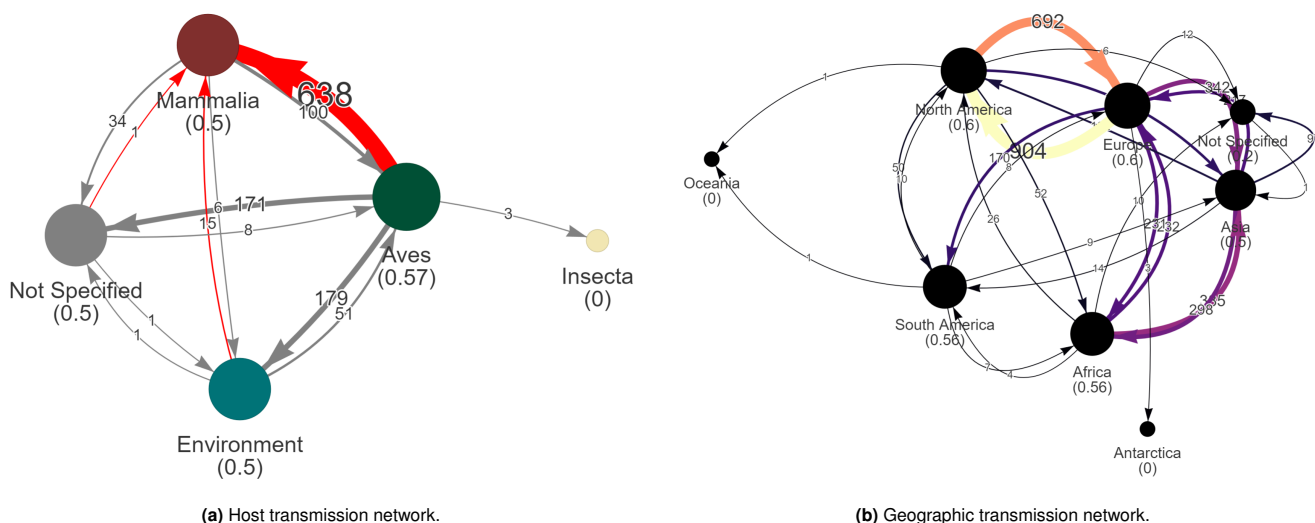


Fig. 2. Transmission networks, generated by StrainHub, showing transmissions between (a) hosts and (b) continents. Node values in parentheses represent the source-hub ratio of that class or location. A source-hub ratio of 1 indicates that the state is always the source of the transmission. The numerical labels annotated on the edges of the graphs represent the number of transmissions as seen across the phylogenetic tree's branches as measured in changes in metadata states.

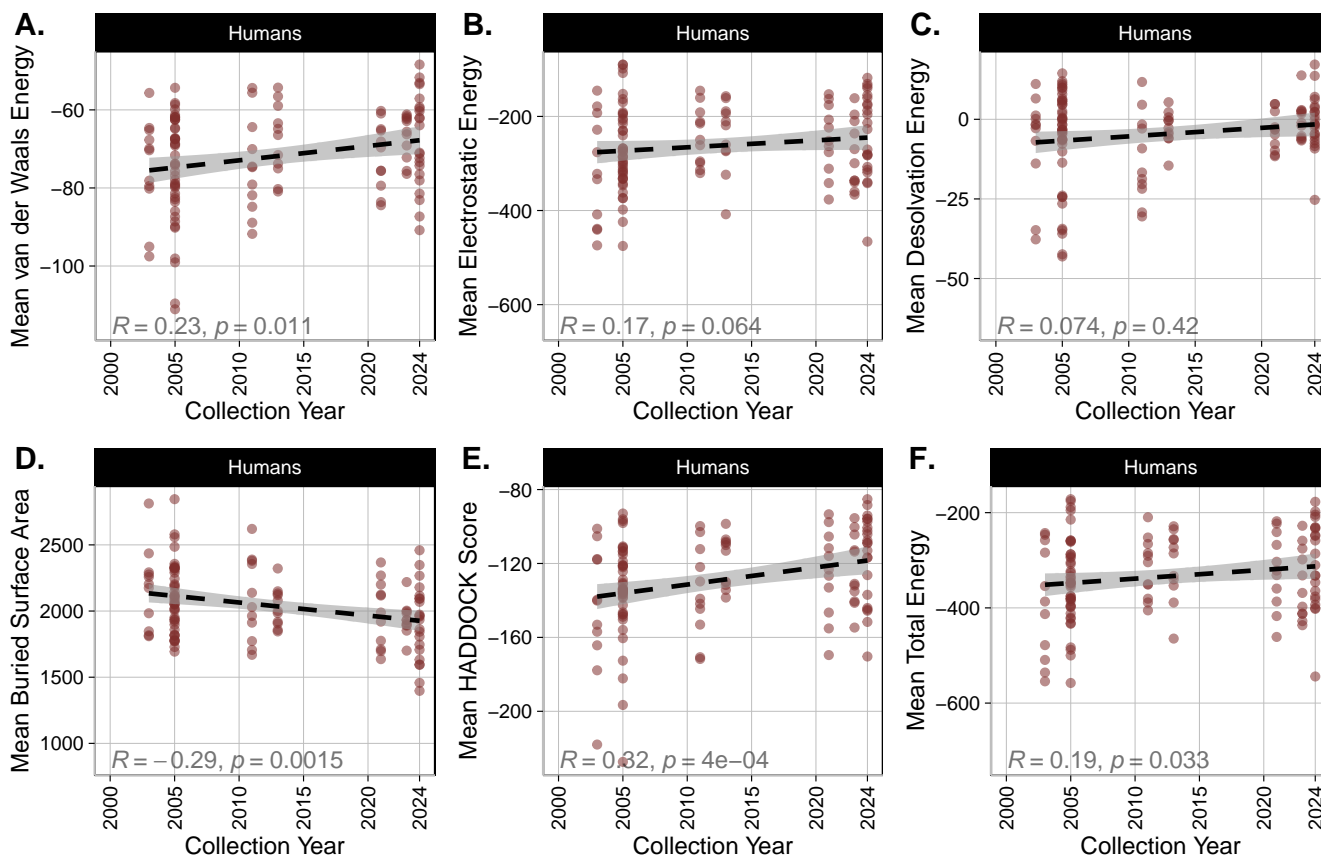


Fig. 3. Antibody binding performance metrics over time for isolates collected from humans. Statistics shown are Spearman correlations. Overall, these plots show a worsening trend in most antibody binding metrics of the human samples.

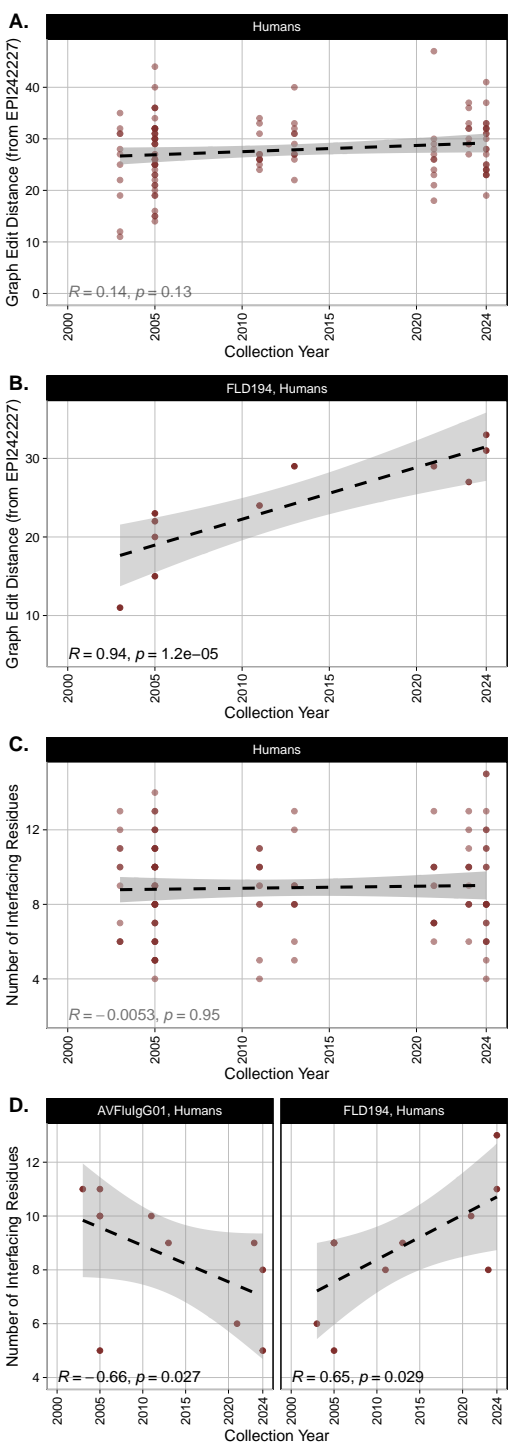


Fig. 4. Graph-based analysis results showing the correlation of the graph edit distance and interfacing residue counts against collection year. Subfigures A and C show the results of all antibodies. Overall, graph edit distance did not change significantly over time. Subfigures B and D show Spearman correlations for specific antibodies of interest. Graph edit distance increased significantly in humans for FLD194. Number of interfacing residues increased in FLD194 in humans.

Diversity of H5N1 Interactions. As shown in Supplementary Figure 3, high disparities in antibody binding affinity exist between different sequences designated as H5N1. For example, in Supplementary Figure 3, sequence EPI597824 has a large disparity in Van der Waals energy between antibody 3C11 and AvFluIG03. In addition, Supplementary Figure 5 demonstrates the effect of a single amino

acid mutation on docking metrics. One change in an amino acid residue can lead to statistically significant differences in antibody binding affinity. These disparities highlight the need to continue to elucidate how differences in amino acid sequences alter binding affinity to various antibodies. Categorizing H5N1 influenza outside of the primary amino acid sequence but on functional binding analyses may yield more effective treatments in the future.

Zoonosis Analysis. In Figure 2a, a notable transition pattern is observed from avian species (class Aves) to mammals (class Mammalia), likely attributable to a mutagenic drift. Recent empirical studies have investigated the mutational dynamics of H5N1, revealing changes in the hemagglutinin (HA) protein. While H5N1 influenza prefers binding to the α 2-3 sialic receptors in birds, this study demonstrated a binding affinity of H5N1 to α 2-6 sialic acid receptors, predominant in mammals, at almost equal proportion (4). These authors also show that mutations that decrease neutralization by sera from mice and ferrets immunized with the vaccine candidate reference strain A/American Wigeon/South Carolina/USDA-000345-001/2021 exist in some of the most recently collected mammalian samples, the dairy cow outbreak starting in April 2024 (4). Concurrently, we show here that mutations accumulated over time in the HA protein will confer reduced neutralization by antibodies more broadly than the current clade 2.3.4.4b H5N1 outbreak.

This *in silico* study aligns with these findings, indicating a progressive decrease in H5N1's binding affinity to antibodies in our isolates over time. As illustrated in Figure 3, there is a marked decline in affinity for human isolates. As the virus diversifies in the avian populations, the potential pool of strains with zoonotic potential to infect mammals increases. The phylogenetic and transmission analysis show much more frequent transmission from avian populations to mammalian populations. This result indicates that much of the evolution is occurring in birds. This suggests an evolutionary trajectory in birds for H5N1 towards increased infection in mammalian hosts with a concomitant immune evasion of the virus in mammals.

Isolate EPI3358339. EPI3358339, a H5N2 subtype isolate, was added to this study as it is from the recent human infection of H5N2 avian influenza seen in Mexico. Unfortunately, this strain was found in a person from Mexico who died of complications due to the infection. However, it is not yet known if the zoonotic “jump” the isolate is cause for concern or if the individual had other comorbidities that played a role in his death. It is also not known if this case is related to recent poultry outbreaks in the area.

The experimental docking conformation between antibodies and this antigen (antibody 65C3 shown in Figure 5F) are predicted to have a relatively strong binding affinity (e.g., Van der Waals energy: [-51.96, -95.45]) across all the tested antibodies.

Thus, our experiments using this isolate's HA do not indicate that this isolate is highly mutated, though some mutations may have reduced the Van der Waals and electrostatic energies of the interaction with this individual's existing antibodies, if any.

Structural Analysis. When comparing the predicted docking outputs to empirical structures, such as those listed in Table 1, we see similar binding epitopes in the the predicted docking complexes versus the empirical structures (42–49).

Furthermore, the binding conformations seen in the empirical structures often mimic the predicted complexes in the experiments in this study, though various mutations affect the binding angle, polar contacts, electrostatics, and overall affinity. These results support the confidence in the predictive accuracy of the *in silico* experiments

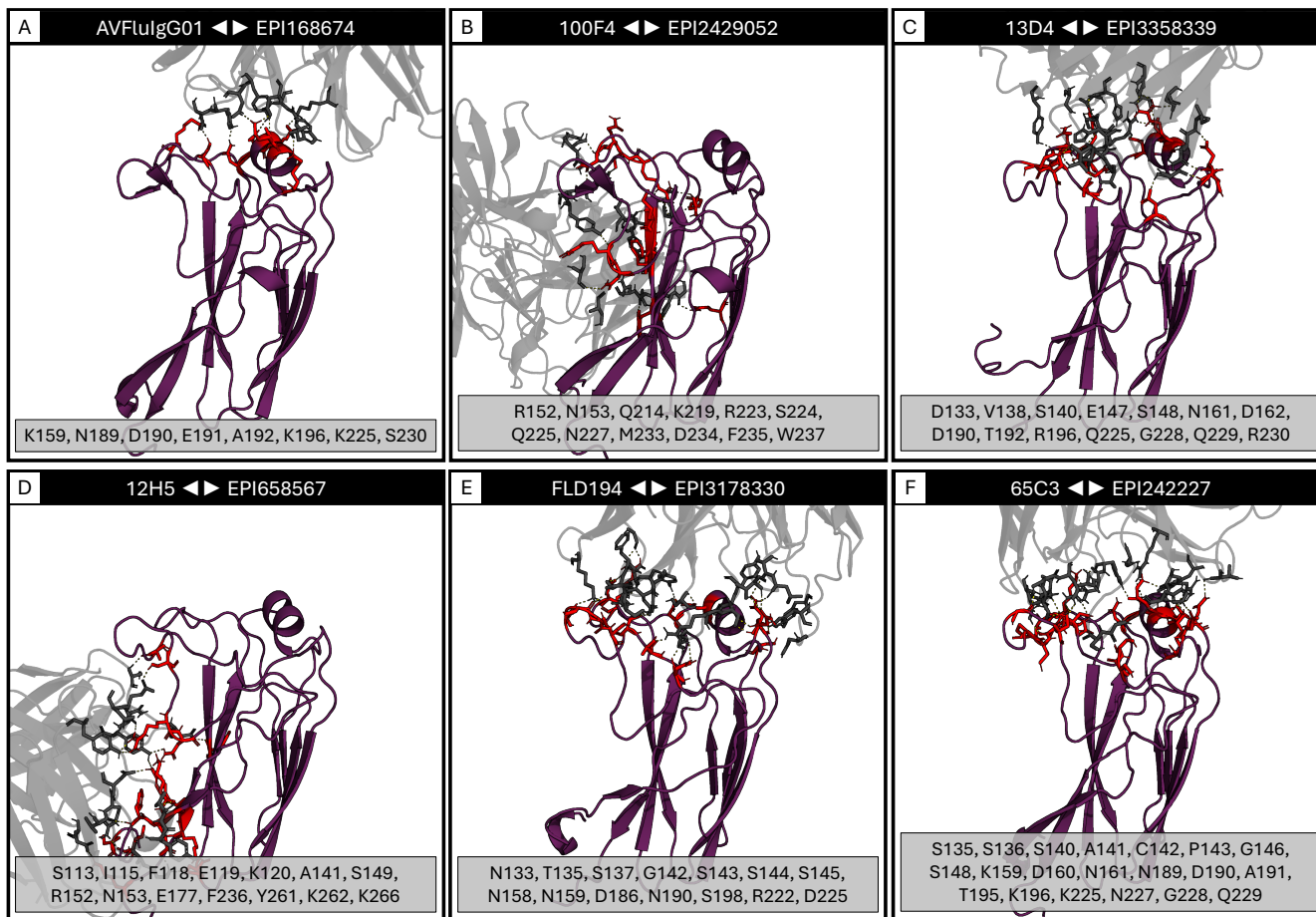


Fig. 5. Example interface renderings showing the diversity in epitopes, residues, and binding affinity. The grey structure is the Fab portion of the docked antibody and the purple structure is the HA1 antigen with sticks designating the polar contacts between them. The list below each subfigure contains the interfacial residues on the antigen chain.

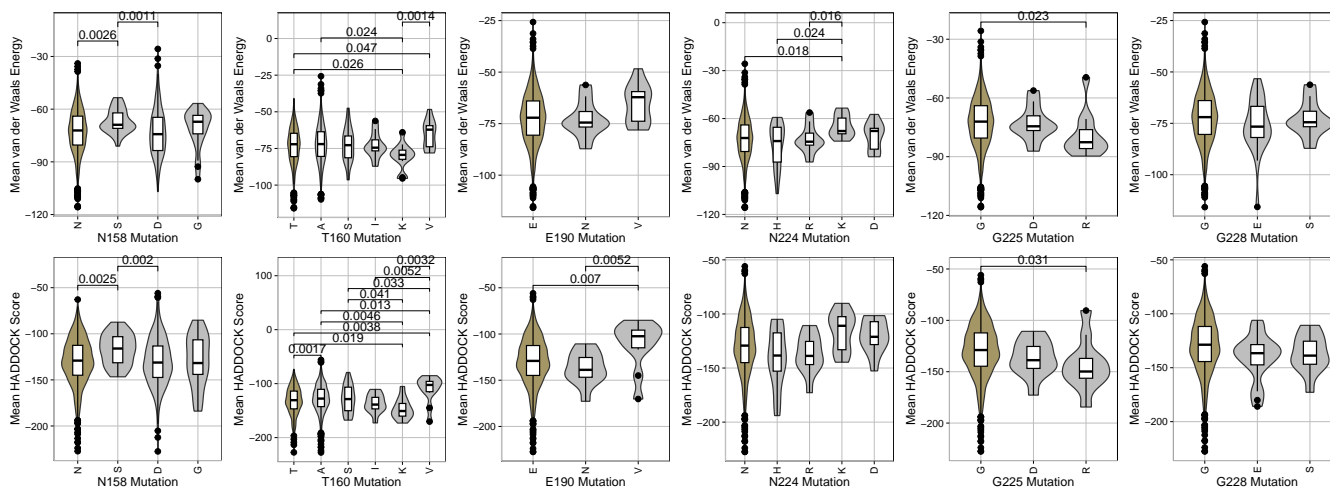


Fig. 6. The distribution of Van der Waals energies and HADDOCK score docking metrics broken out by antigen mutations. The first amino acid shown on the left of each plot in gold represents the reference residue at that position as described in [Shi et al. \(2014\)](#). Statistical comparisons shown are significant Wilcoxon Rank Sum test p-values at the $\alpha < 0.05$ level.

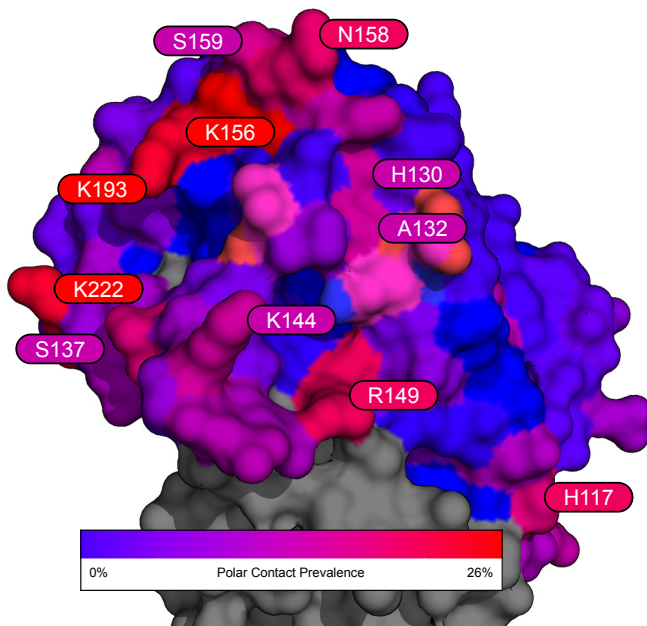


Fig. 7. Surface rendering of the HA1 globular head domain (reference PDB 2FK0) showing the prevalence of each residue to form polar contacts (within 3Å of antibody residues) across the experiments in this study. Annotated residues are those with $\geq 16\%$ prevalence.

given their similarity to empirically derived structures. However, empirical studies are still needed to validate specific complexes.

Motifs of Interest and Future Research. H5N1 exists as an endemic in avian populations. This endemic creates a pool containing vast numbers of host species in which the RNA virus evolves rapidly. It is an endemic that is difficult to diminish due to the nature of the HA protein's host receptors lacking homogeneity. Serological immunity from vaccination or prior infection in avian hosts may have yielded selective pressures in the evolution of specific mechanisms of entry for H5N1 (65). Subsequently, high infection rates lead to new mechanisms of entry. Over time, serological immunity from original vaccination and/or infection is reduced, and the cycle of influenza transmission continues.

Highly conserved portions of HA are of high interest. The three primary conserved elements of the receptor-binding site (RBS) on the HA1 subunit are the 130 and 220-loops and the 190-helix (66–68). As shown in Figures 5 and 7, the antibodies docked to conserved motifs on the studied H5N1 strains, further supporting the empirical literature that initially identified their neutralizing capability.

More recent development of multivalent mRNA-based vaccines has been successful in H5 influenza A clade 2.3.4.4b (from which there are 15 sequences used in the structural aspects of this study) (69). The selection of high-quality sequences that elicit strong antibody responses is a complex process in mRNA vaccine development. However, *in silico* modeling, as presented in this study, reduces the wet laboratory workload to evaluate candidate sequences from which vaccines can be developed.

In addition, our broad analyses of various antibodies versus strains of interest may guide future therapeutic antibody development. Antibodies tested within this study, particularly those with high affinity to studied strains that may bear high homology to those that will arise in the future, can be used as a basis for future pharmaceutical development.

Computational modeling of immunoprotein interactions as

shown in this study and previous works (24–29) have proven to be highly effective in the prompt prediction and understanding of the health impacts of pathogen variants. For H5 influenza, this study, along with recent preprints (18, 70), show an overall trend of worsening antibody binding and depicts the recent increase in avian-to-mammalian transmissions due to various mutations. This suggests that there is an impending danger to human health for highly pathogenic strains of H5 influenza that can infect avian and mammalian livestock and jump to humans.

More broadly, these results indicate that the virus has potential to move from epidemic to pandemic status in the near future. "Pandemic" here refers to the geographic spread of a virus, which H5N1 has already achieved, but these results more specifically assert that the worsening trend of the antibody performance along with the already present animal pandemic is a cause for concern for an eventual human pandemic.

Contributors

Authors SY, KO, and SGM retrieved the H5 antigen sequences from GISAID and antibody structures from Protein Data Bank. SY performed the structure prediction of the antigens. Author RAW performed the clustering analysis. Authors KO and CTF curated the metadata of the H5 sequences. Author DJ performed the phylogenetic analyses. Authors SY and CTF performed the protein structure analyses. Author PJT performed the multiple sequence alignment. Author RJ3 performed the graph-edit distance analysis. Author CTF performed the docking experiments and statistical analyses and generated all figures. All authors wrote and reviewed the manuscript.

Declaration of Interests

Author CTF is the owner of Tuple, LLC, a biotechnology consulting firm. The remaining authors declare that the research was conducted in the absence of any commercial or financial relationships that could be construed as a potential conflict of interest.

Acknowledgements

We gratefully acknowledge all GISAID data contributors (i.e., the authors and their originating laboratories) responsible for obtaining the specimens, and their submitting laboratories for generating the genetic sequence and metadata and sharing via the GISAID Initiative, on which this research is based.

We acknowledge the following entities at the University of North Carolina at Charlotte: Academic Affairs, The Office of Research, The Center for Computational Intelligence to Predict Health and Environmental Risks (CIPHER), The Department of Bioinformatics and Genomics, The College of Computing and Informatics, and the University Research Computing group. We gratefully acknowledge the support of the Belk Family.

Data Sharing Statement

All code, data, results, and additional analyses are openly available on GitHub at: https://github.com/colbyford/Influenza_H5-Antibody_Predictions. These data include all sequences and folded structures for the isolates and antibodies used in this study, analysis scripts, and docking metrics.

Funding Statement

No external funding was used for this study.

Bibliography

1. USDA Animal and Plant Health Inspection Service. USDA APHIS Livestock and Poultry Health: Avian Influenza High Pathogenicity Avian Influenza Detections in Mammals. <https://www.aphis.usda.gov/livestock-poultry-disease/avian/avian-influenza/hpai-detections/mammals>, 2024. Accessed: 2024-06-20.
2. CDC. H5 Bird Flu: Current Situation. <https://www.cdc.gov/bird-flu/situation-summary/index.html>, October 2024. Accessed: 2024-10-23.
3. Yi Shi, Ying Wu, Wei Zhang, Jianxun Qi, and George F. Gao. Enabling the 'host jump': structural determinants of receptor-binding specificity in influenza A viruses. *Nature Reviews Microbiology*, 12(12):822–831, Dec 2014. ISSN 1740-1534. doi: 10.1038/nrmicro3362.
4. Bernadeta Dadonaite, Jenny J. Ahn, Jordan T. Ort, Jin Yu, Colleen Furey, Annie Dosey, William W. Hannon, Amy L. Vincent Baker, Richard Webby, Neil P. King, Yan Liu, Scott E. Hensley, Thomas P. Peacock, Louise H. Moncla, and Jesse D. Bloom. Deep mutational scanning of h5 hemagglutinin to inform influenza virus surveillance. *bioRxiv*, 2024. doi: 10.1101/2024.05.23.595634.
5. R G Webster, W J Bean, O T Gorman, T M Chambers, and Y Kawaoka. Evolution and ecology of influenza A viruses. *Microbiological Reviews*, 56(1):152–179, 1992. doi: 10.1128/mr.56.1.152-179.1992.
6. Daniel Janies, Andrew W Hill, Robert Guralnick, Farhat Habib, Eric Waltari, and Ward C Wheeler. Genomic Analysis and Geographic Visualization of the Spread of Avian Influenza (H5N1). *Systematic Biology*, 56(2):321–329, 04 2007. ISSN 1063-5157. doi: 10.1080/10635150701266848.
7. Centers for Disease Control and Prevention. Avian Influenza Timeline: 1880-1959. <https://www.cdc.gov/bird-flu/avian-timeline/1880-1959.html>, 2023. Accessed: 2024-10-31.
8. Kennedy F. Shortridge. Influenza - a continuing detective story. *The Lancet*, 354:SIV29, Dec 1999. ISSN 0140-6736. doi: 10.1016/S0140-6736(99)90372-0.
9. The New York Times. Hong kong culls chickens after bird flu is found. *The New York Times*, 2011. Accessed: 2024-06-25.
10. Stephanie Sonnberg, Richard J. Webby, and Robert G. Webster. Natural history of highly pathogenic avian influenza h5n1. *Virus Research*, 178(1):63–77, 2013. ISSN 0168-1702. doi: <https://doi.org/10.1016/j.virusres.2013.05.009>. H5N1.
11. Steven L. Salzberg, Carl Kingsford, Giovanni Cattoli, David J. Spiro, Daniel A. Janies, Magdi M. Aly, and Ilaria Capua. Genome Analysis Linking Recent European and African Influenza (H5N1) Viruses. *Emerging Infectious Diseases*, 13(5):713, 2007. doi: 10.3201/eid1305.070013.
12. World Health Organization. Influenza Virus Infections in Humans. <https://www.who.int/publications/m/item/influenza-virus-infections-in-humans>, February 2014. Accessed: 2024-06-25.
13. WHO. Influenza A(H5N1) highly pathogenic avian influenza: timeline of major events. [https://www.who.int/publications/m/item/influenza-a\(h5n1\)-highly-pathogenic-avian-influenza-timeline-of-major-events](https://www.who.int/publications/m/item/influenza-a(h5n1)-highly-pathogenic-avian-influenza-timeline-of-major-events), December 2014. Accessed: 2024-08-02.
14. Javad Charostad, Mohammad Rezaei Zadeh Rukerd, Shahab Mahmoudvand, Davood Bashash, Seyed Mohammad Ali Hashemi, Mohsen Nakhaie, and Keivan Zandi. A comprehensive review of highly pathogenic avian influenza (HPAI) H5N1: An imminent threat at doorstep. *Travel Medicine and Infectious Disease*, 55:102638, 2023. ISSN 1477-8939. doi: <https://doi.org/10.1016/j.tmaid.2023.102638>.
15. ABC News. Bird Flu Mutation Reaches Antarctica, Sparks Australia Outbreak. <https://www.abc.net.au/news/2024-05-21/bird-flu-mutation-reaches-antarctica-australia-outbreak/103844240>, May 2024. Accessed: 2024-06-25.
16. Features of H5N1 influenza viruses in dairy cows may facilitate infection, transmission in mammals, Jul 2024.
17. ER Burrough, DR Magstadt, B Petersen, SJ Timmermans, PC Gauger, J Zhang, C Siepker, M Mainenti, G Li, A Thompson, P Gorden, P Plummer, and R Main. Highly Pathogenic Avian Influenza A(H5N1) Clade 2.3.4.4b Virus Infection in Domestic Dairy Cattle and Cats, United States, 2024. *Emerging Infectious Diseases*, 2024. doi: 10.3201/eid3007.240508.
18. Leonardo C. Caserta, Elisha A. Frye, Salmaan L. Butt, Melissa Laverack, Mohammed Nooruzaman, Lina M. Covaldea, Alexis C. Thompson, Melanie Prarat Koscielny, Brittany Cronk, Ashley Johnson, Katie Kleinhenz, Erin E. Edwards, Gabriel Gomez, Gavin Hitchcher, Mathias Martins, Darrell R. Kapczynski, David L. Suarez, Ellen Ruth Alexander Morris, Terry Hensley, John S. Beeby, Manigandan Lejeune, Amy K. Swinford, François Elvinger, Kiril M. Dimitrov, and Diego G. Diel. Spillover of highly pathogenic avian influenza h5n1 virus to dairy cattle. *Nature*, Jul 2024. ISSN 1476-4687. doi: 10.1038/s41586-024-07849-4.
19. Shikha Garg. Outbreak of highly pathogenic avian influenza A (H5N1) viruses in US dairy cattle and detection of two human cases—United States, 2024. *MMWR. Morbidity and Mortality Weekly Report*, 73, 2024.
20. Falguni Debnath, Debjit Chakraborty, Alok Kumar Deb, Malay Kumar Saha, and Shanta Datta. Increased human-animal interface & emerging zoonotic diseases: An enigma requiring multi-sectoral efforts to address. *Indian Journal of Medical Research*, 153(5-6):577–584, 2021.
21. Centers for Disease Control and Prevention (CDC). CDC Media Release: CDC to Provide Vaccine Candidate Viruses to Better Protect Against Avian Influenza. <https://www.cdc.gov/media/releases/2024/p0401-avian-flu.html>, 2024. Accessed: 2024-07-13.
22. Centers for Disease Control and Prevention (CDC). CDC A(H5N1) Bird Flu Response Update June 14, 2024. <https://www.cdc.gov/bird-flu/spotlights/h5n1-response-06142024.html>, 2024. Accessed: 2024-08-3.
23. Smriti Mallapaty. Bird flu could become a human pandemic. How are countries preparing? *Nature*, July 2024. doi: 10.1038/d41586-024-02237-4.
24. Phillip J. Tomezsko, Colby T. Ford, Avery E. Meyer, Adam M. Michaleas, and Rafael Jaimés. Human cytokine and coronavirus nucleocapsid protein interactivity using large-scale virtual screens. *Frontiers in Bioinformatics*, 4, 2024. ISSN 2673-7647. doi: 10.3389/fbinf.2024.1397968.
25. Colby T. Ford. PD-1 Targeted Antibody Discovery Using AI Protein Diffusion. *Technology in Cancer Research & Treatment*, 2024. doi: 10.1177/15330338241275947.
26. Shirish Yasa, Sayal Guirales-Medrano, Denis Jacob Machado, Colby T. Ford, and Daniel A. Janies. Predicting Antibody and ACE2 Affinity for SARS-CoV-2 BA.2.86 and JN.1 with *In Silico* Protein Modeling and Docking. *Frontiers in Virology*, 4, 2024. ISSN 2673-818X. doi: 10.3389/fviro.2024.1419276.
27. Colby T. Ford, Shirish Yasa, Denis Jacob Machado, Richard Allen White III, and Daniel A. Janies. Predicting changes in neutralizing antibody activity for SARS-CoV-2 XBB.1.5 using *in silico* protein modeling. *Frontiers in Virology*, 3, 2023. ISSN 2673-818X. doi: 10.3389/fviro.2023.1172027.
28. Colby T. Ford, Denis Jacob Machado, and Daniel A. Janies. Predictions of the SARS-CoV-2 Omicron Variant (B.1.1.529) Spike Protein Receptor-Binding Domain Structure and Neutralizing Antibody Interactions. *Frontiers in Virology*, 2022. doi: 10.3389/fviro.2022.830202.
29. Cheikh Cambel Dieng, Colby T. Ford, Anita Lerch, Dickson Donioug, Kovidh Vegesna, Daniel Janies, Liwang Cui, Linda Amoah, Yaw Afrane, and Eugenia Lo. Genetic variations of *Plasmodium falciparum* circumsporozoite protein and the impact on interactions with human immunoproteins and malaria vaccine efficacy. *Infection, Genetics and Evolution*, 2023. ISSN 1567-1348. doi: <https://doi.org/10.1016/j.meegid.2023.105418>.
30. Yuelong Shu and John McCauley. GISAID: Global initiative on sharing all influenza data – from vision to reality. *Eurosurveillance*, 22(13):30494, 2017. doi: <https://doi.org/10.2807/1560-7917.ES.2017.22.13.30494>.
31. Stefan Elbe and Gemma Buckland-Merrett. Data, disease and diplomacy: GISAID's innovative contribution to global health. *Global Challenges*, 1(1):33–46, 2017. doi: <https://doi.org/10.1002/gch2.1018>.
32. Weizhong Li and Adam Godzik. CD-HIT: a fast program for clustering and comparing large sets of protein or nucleotide sequences. *Bioinformatics*, 22(13):1658–1659, 05 2006. ISSN 1367-4803. doi: 10.1093/bioinformatics/btl158.
33. Limin Fu, Beifang Niu, Zhengwei Zhu, Sitao Wu, and Weizhong Li. CD-HIT: accelerated for clustering the next-generation sequencing data. *Bioinformatics*, 28(23):3150–3152, 10 2012. ISSN 1367-4803. doi: 10.1093/bioinformatics/bts565.
34. Robert C. Edgar. MUSCLE: multiple sequence alignment with high accuracy and high throughput. *Nucleic Acids Research*, 32(5):1792–1797, 03 2004. ISSN 0305-1048. doi: 10.1093/nar/gkh340.
35. Nongluk Sriwilajjaroen and Yasuo Suzuki. Molecular basis of the structure and function of H1 hemagglutinin of influenza virus. *Proceedings of the Japan Academy, Series B*, 88(6): 226–249, 2012. doi: 10.2183/pjab.88.226.
36. Milot Mirdita, Konstantin Schütze, Yoshitaka Moriwaki, Lim Heo, Sergey Ovchinnikov, and Martin Steinegger. ColabFold: making protein folding accessible to all. *Nature Methods*, 19(6):679–682, Jun 2022. ISSN 1548-7105. doi: 10.1038/s41592-022-01488-1.
37. John Jumper, Richard Evans, Alexander Pritzel, Tim Green, Michael Figurnov, Olaf Ronenberger, Kathryn Tunyasuvunakool, Russ Bates, Augustin Židek, Anna Potapenko, Alex Bridgland, Clemens Meyer, Simon A. A. Kohl, Andrew J. Baillard, Andrew Cowie, Bernardino Romera-Paredes, Stanislaw Nikolov, Rishub Jain, Jonas Adler, Trevor Back, Stig Petersen, David Reiman, Ellen Clancy, Michal Zieliński, Martin Steinegger, Michalina Pacholska, Tamas Berghammer, Sebastian Bodenstein, David Silver, Oriol Vinyals, Andrew W. Senior, Koray Kavukcuoglu, Pushmeet Kohli, and Demis Hassabis. Highly accurate protein structure prediction with alphafold. *Nature*, 596(7873):583–589, Aug 2021. ISSN 1476-4687. doi: 10.1038/s41586-021-03819-2.
38. Martin Steinegger and Johannes Söding. MMseqs2 enables sensitive protein sequence searching for the analysis of massive data sets. *Nature Biotechnology*, 35(11):1026–1028, Nov 2017. ISSN 1546-1696. doi: 10.1038/nbt.3988.
39. Peter Eastman, Jason Swails, John D. Chodera, Robert T. McGibbon, Yutong Zhao, Kyle A. Beauchamp, Lee-Ping Wang, Andrew C. Simmonett, Matthew P. Harrigan, Chaya D. Stern, Rafal P. Wiewiora, Bernard R. Brooks, and Vijay S. Pande. Openmm 7: Rapid development of high performance algorithms for molecular dynamics. *PLOS Computational Biology*, 13(7):1–17, 07 2017. doi: 10.1371/journal.pcbi.1005659.
40. Matthew I J Raybould, Claire Marks, Alan P Lewis, Jiye Shi, Alexander Bujotzek, Bruck Taddeas, and Charlotte M Deane. Thera-SABDab: the Therapeutic Structural Antibody Database. *Nucleic Acids Research*, 48(D1):D383–D388, 09 2019. ISSN 0305-1048. doi: 10.1093/nar/gkz827.
41. Helen M. Berman, John Westbrook, Zukang Feng, Gary Gilliland, T. N. Bhat, Helge Weissig, Ilya N. Shindyalov, and Philip E. Bourne. The Protein Data Bank. *Nucleic Acids Research*, 28(1):235–242, 01 2000. ISSN 0305-1048. doi: 10.1093/nar/28.1.235.
42. Teng Zuo, Jianfeng Sun, Guiqin Wang, Liwei Jiang, Yanan Zuo, Danyang Li, Xuanliang Shi, Xi Liu, Shilong Fan, Huanhuan Ren, Hongxing Hu, Lina Sun, Boping Zhou, Mifang Liang, Paul Zhou, Xinquan Wang, and Linqi Zhang. Comprehensive analysis of antibody recognition in convalescent humans from highly pathogenic avian influenza h5n1 infection. *Nature Communications*, 6(1):8855, Dec 2015. ISSN 2041-1723. doi: 10.1038/ncomms9855.
43. Tingting Li, Junyu Chen, Qingbing Zheng, Wenhui Xue, Limin Zhang, Rui Rong, Sibao Zhang, Qiang Wang, Mingqing Hong, Yuyun Zhang, Lingyan Cui, Maozhou He, Zhen Lu, Zhenyong Zhang, Xin Chi, Jinjin Li, Yang Huang, Hong Wang, Jixian Tang, Dong Ying, Lizhi Zhou, Yingbin Wang, Hai Yu, Jun Zhang, Ying Gu, Yixin Chen, Shaowei Li, and Ningshao Xia. Identification of a cross-neutralizing antibody that targets the receptor binding site of h1n1 and h5n1 influenza viruses. *Nature Communications*, 13(1):5182, Sep 2022. ISSN 2041-1723. doi: 10.1038/s41467-022-32926-5.
44. Qingshan Lin, Tingting Li, Yixin Chen, Siu-Ying Lau, Minxi Wei, Yuyun Zhang, Zhenyong Zhang, Qiaobin Yao, Jinjin Li, Zhihai Li, Daning Wang, Qingbing Zheng, Hai Yu, Ying Gu, Jun Zhang, Honglin Chen, Shaowei Li, and Ningshao Xia. Structural basis for the broad, antibody-mediated neutralization of h5n1 influenza virus. *Journal of Virology*, 92(17):10.1128/jvi.00547-18, 2018. doi: 10.1128/jvi.00547-18.
45. Pengfei Wang, Yanan Zuo, Jianfeng Sun, Teng Zuo, Senyan Zhang, Shichun Guo, Xuanliang Shi, Mifang Liang, Paul Zhou, Linqi Zhang, and Xinquan Wang. Structural and functional definition of a vulnerable site on the hemagglutinin of highly pathogenic avian influenza a virus h5n1. *Journal of Biological Chemistry*, 294(12):4290–4303, Mar 2019. ISSN 0021-9258. doi: 10.1074/jbc.RA118.007008.
46. Xiaoli Xiong, Davide Corti, Junfeng Liu, Debora Pinna, Mathilde Foglierini, Lesley J. Calder, Stephen R. Martin, Yi Pu Lin, Philip A. Walker, Patrick J. Collins, Isabella Monne, Amoroso L. Suguitan, Celia Santos, Nigel J. Temperton, Kanta Subbarao, Antonio Lanza-vecchia, Steven J. Gamblin, and John J. Skehel. Structures of complexes formed by

- h5 influenza hemagglutinin with a potent broadly neutralizing human monoclonal antibody. *Proceedings of the National Academy of Sciences*, 112(30):9430–9435, 2015. doi: 10.1073/pnas.1510816112.
47. Yanan Zuo, Pengfei Wang, Jianfeng Sun, Shichun Guo, Guiqin Wang, Teng Zuo, Shilong Fan, Paul Zhou, Mifang Liang, Xuanling Shi, Xinquan Wang, and Linqi Zhang. Complementary recognition of the receptor-binding site of highly pathogenic h5n1 influenza viruses by two human neutralizing antibodies. *Journal of Biological Chemistry*, 293(42):16503–16517, Oct 2018. ISSN 0021-9258. doi: 10.1074/jbc.RA118.004604.
48. Xueyong Zhu, Yong-Hui Guo, Tao Jiang, Ya-Di Wang, Kwok-Hung Chan, Xiao-Feng Li, Wenli Yu, Ryan McBride, James C. Paulson, Kwok-Yung Yuen, Cheng-Feng Qin, Xiao-Yan Che, and Ian A. Wilson. A unique and conserved neutralization epitope in h5n1 influenza viruses identified by an antibody against the a/goose/guangdong/1/96 hemagglutinin. *Journal of Virology*, 87(23):12619–12635, 2013. doi: 10.1128/jvi.01577-13.
49. Katie L. Winarski, Natalie J. Thornburg, Yingchun Yu, Gopal Sapparapu, James E. Crowe, and Benjamin W. Spiller. Vaccine-elicited antibody that neutralizes h5n1 influenza and variants binds the receptor site and polymorphic sites. *Proceedings of the National Academy of Sciences*, 112(30):9346–9351, 2015. doi: 10.1073/pnas.1502762112.
50. G.C.P. van Zundert, J.P.G.L.M. Rodrigues, M. Trellet, C. Schmitz, P.L. Kastriitis, E. Karaca, A.S.J. Melquioid, M. van Dijk, S.J. de Vries, and A.M.J.J. Bonvin. The HADDOCK2.2 Web Server: User-Friendly Integrative Modeling of Biomolecular Complexes. *Journal of Molecular Biology*, 428(4):720–725, 2016. doi: 10.1016/j.jmb.2015.09.014.
51. James Dunbar and Charlotte M. Deane. ANARCI: antigen receptor numbering and receptor classification. *Bioinformatics*, 32(2):298–300, 09 2015. ISSN 1367-4803. doi: 10.1093/bioinformatics/btv552.
52. Bonvin Lab. HADDOCK3 Antibody-Antigen Tutorial. <https://www.bonvinlab.org/education/HADDOCK3/HADDOCK3-antibody-antigen/>, 2024. Accessed: 2024-06-21.
53. João P. G. L. M. Rodrigues, Mikaël Trellet, Christophe Schmitz, Panagiotis Kastriitis, Ezgi Karaca, Adrien S. J. Melquioid, and Alexandre M. J. J. Bonvin. Clustering biomolecular complexes by residue contacts similarity. *Proteins: Structure, Function, and Bioinformatics*, 80(7):1810–1817, 2012. doi: <https://doi.org/10.1002/prot.24078>.
54. Kazutaka Katoh and Daron M. Standley. MAFFT Multiple Sequence Alignment Software Version 7: Improvements in Performance and Usability. *Molecular Biology and Evolution*, 30(4):772–780, 01 2013. ISSN 0737-4038. doi: 10.1093/molbev/mst010.
55. Pablo A. Goloboff and Martin E. Morales. TNT version 1.6, with a graphical interface for MacOS and Linux, including new routines in parallel. *Cladistics*, 39(2):144–153, 2023. doi: <https://doi.org/10.1111/cla.12524>.
56. Adriano de Bernardi Schneider, Colby T Ford, Reilly Hostager, John Williams, Michael Ciocco, Ümit V Çatalyürek, Joel O Wertheim, and Daniel Janies. StrainHub: A phylogenetic tool to construct pathogen transmission networks. *Bioinformatics*, 08 2019. ISSN 1367-4803. doi: 10.1093/bioinformatics/btz646.
57. R Core Team. *R: A Language and Environment for Statistical Computing*. R Foundation for Statistical Computing, Vienna, Austria, 2021.
58. Hadley Wickham. *ggplot2: Elegant Graphics for Data Analysis*. Springer-Verlag New York, 2016. ISBN 978-3-319-24277-4.
59. Albukadel Kassambara. *ggpubr: 'ggplot2' Based Publication Ready Plots*, 2023. R package version 0.6.0.
60. Schrödinger, LLC. The PyMOL molecular graphics system. version 2.4.1, November 2015.
61. Sebastian Raschka. BioPandas: Working with molecular structures in pandas DataFrames. *The Journal of Open Source Software*, 2(14), jun 2017. doi: 10.21105/joss.00279.
62. Giovanni Cattoli, Adelaide Milani, Nigel Temperton, Bianca Zecchin, Alessandra Buratin, Eleonora Molesti, Mona Mehrez Aly, Abdel Arafa, and Ilaria Capua. Antigenic drift in H5N1 avian influenza virus in poultry is driven by mutations in major antigenic sites of the hemagglutinin molecule analogous to those for human influenza virus. *Journal of virology*, 85(17):8718–8724, 2011.
63. Christian Grund, El-Sayed M Abdelwhab, Abdel-Satar Arafa, Mario Ziller, Mohamed K Hassan, Mona M Aly, Hafez M Hafez, Timm C Harder, and Martin Beer. Highly pathogenic avian influenza virus H5N1 from Egypt escapes vaccine-induced immunity but confers clinical protection against a heterologous clade 2.2. 1 Egyptian isolate. *Vaccine*, 29(33):5567–5573, 2011.
64. O Munoz, M De Nardi, K van der Meulen, K van Reeth, M Koopmans, K Harris, S von Dobschütz, G Freidl, A Meijer, A Breed, A Hill, R Kosmider, J Banks, K Stark, B Wieland, K Stevens, S van der Werf, V Enouf, G Dauphin, W Dundon, G Cattoli, I Capua, and the FLURISK Consortium. Genetic adaptation of influenza A viruses in domestic animals and their potential role in interspecies transmission: A literature review. *EcoHealth*, 13:171–198, 2015. doi: 10.1007/s10393-014-1004-1.
65. Huaiyu Tian, Yujun Cui, Lu Dong, Sen Zhou, Xiaowen Li, Shanqian Huang, Ruiyu Yang, and Bing Xu. Spatial, temporal and genetic dynamics of highly pathogenic avian influenza A (H5N1) virus in China. *BMC Infectious Diseases*, 15(1):54, Feb 2015. ISSN 1471-2334. doi: 10.1186/s12879-015-0770-x.
66. John J Skehel and Don C Wiley. Receptor binding and membrane fusion in virus entry: the influenza hemagglutinin. *Annual review of biochemistry*, 69(1):531–569, 2000.
67. Ya Ha, David J Stevens, John J Skehel, and Don C Wiley. X-ray structures of H5 avian and H9 swine influenza virus hemagglutinins bound to avian and human receptor analogs. *Proceedings of the National Academy of Sciences*, 98(20):11181–11186, 2001.
68. Netanel Tzarum, Robert P De Vries, Xueyong Zhu, Wenli Yu, Ryan McBride, James C Paulson, and Ian A Wilson. Structure and receptor binding of the hemagglutinin from a human H6N1 influenza virus. *Cell host & microbe*, 17(3):369–376, 2015.
69. Colleen Furey, Gabrielle Scher, Naiqing Ye, Lisa Kercher, Jennifer DeBeauchamp, Jeri Carol Crumpton, Trushar Jeevan, Christopher Patton, John Franks, Adam Rubrum, Mohamad-Gabriel Alameh, Steven H. Y. Fan, Anthony T. Phan, Christopher A. Hunter, Richard J. Webby, Drew Weissman, and Scott E. Hensley. Development of a nucleoside-modified mRNA vaccine against clade 2.3.4.4b H5 highly pathogenic avian influenza virus. *Nature Communications*, 15(1):4350, May 2024. ISSN 2041-1723. doi: 10.1038/s41467-024-48555-z.
70. Bernadeta Dadonaite, Jenny J. Ahn, Jordan T. Ort, Jin Yu, Colleen Furey, Annie Dosey,

Supplementary Information

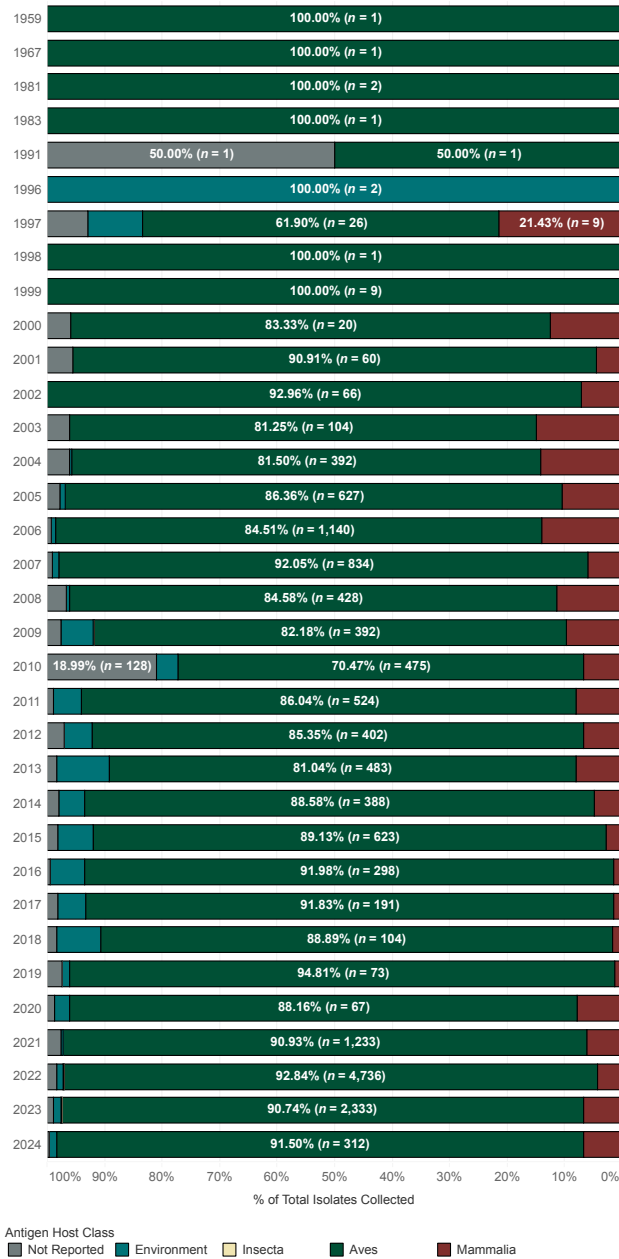


Fig. 1. Bar chart of the proportion of isolates collected from hosts of various taxonomic classes by year.

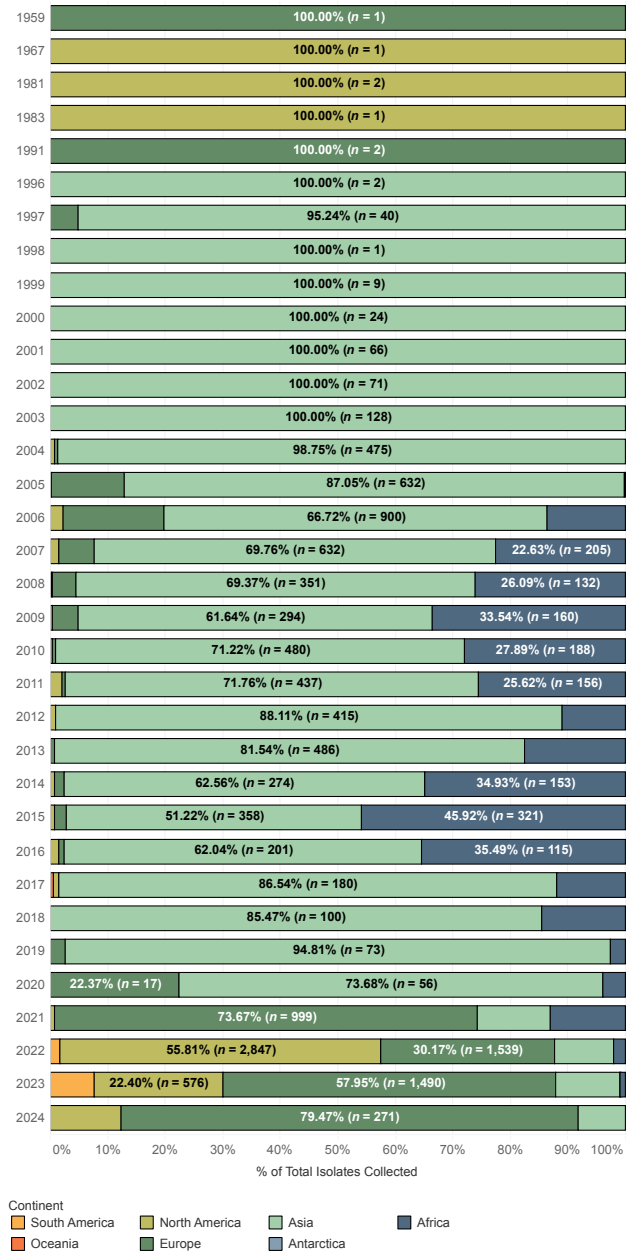


Fig. 2. Bar chart of the proportion of isolates collected from each continent by year.

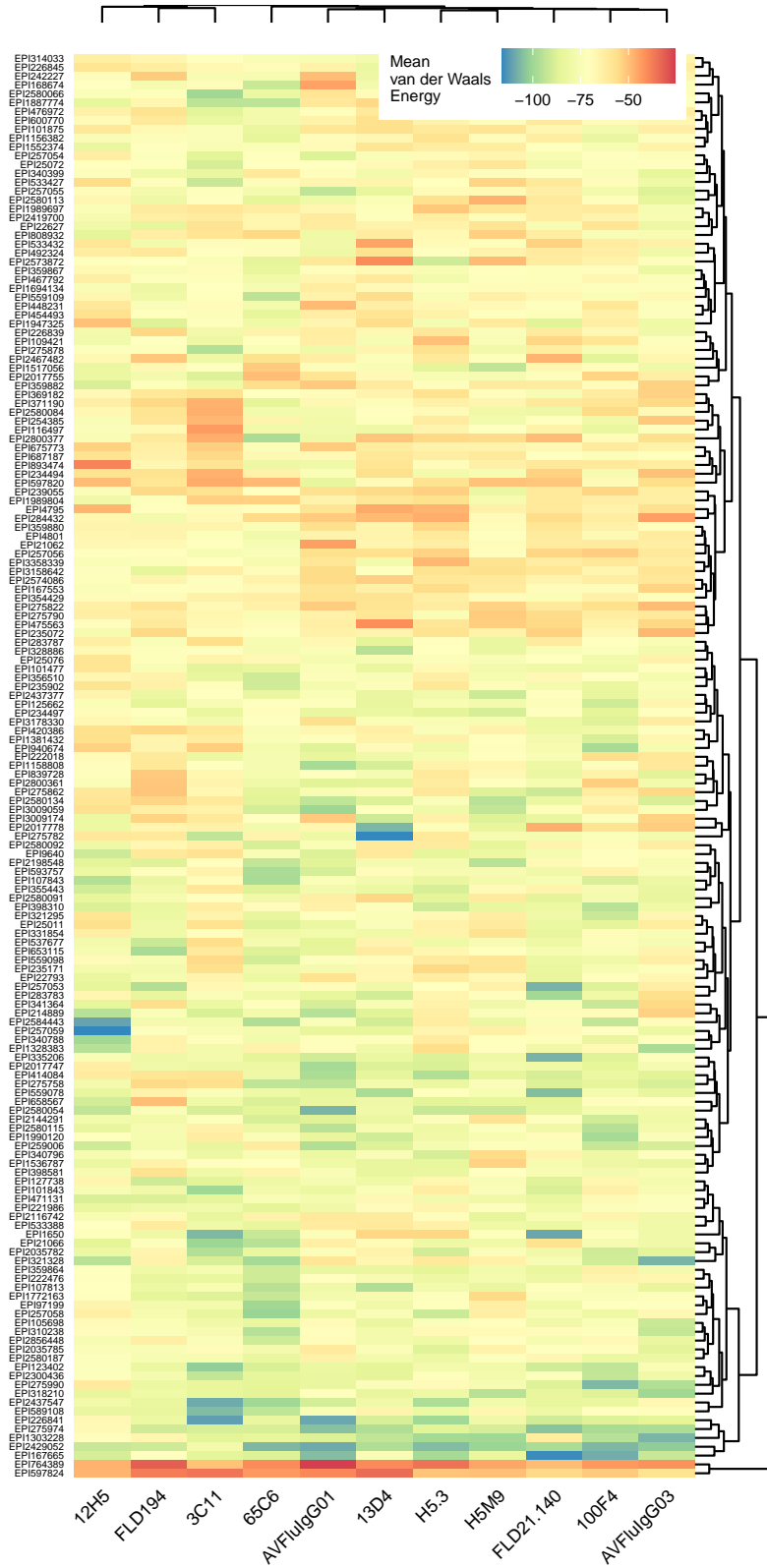


Fig. 3. Heatmap of van der Waals energies for each antibody-antigen experiment, shown with cluster dendrograms.

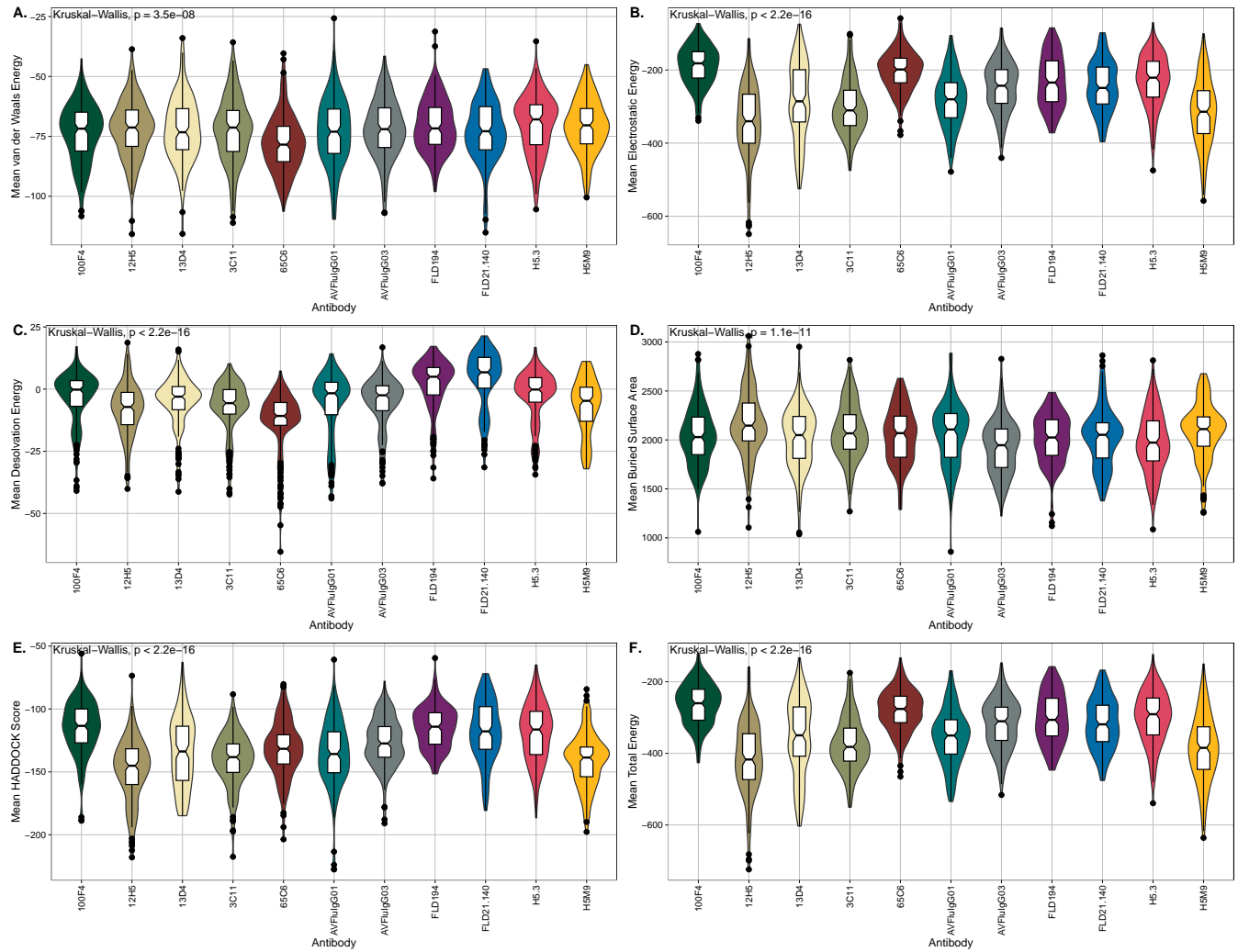


Fig. 4. The distribution of various docking metrics broken out by antibody. Statistics shown are Kruskal-Wallis test p-values.

